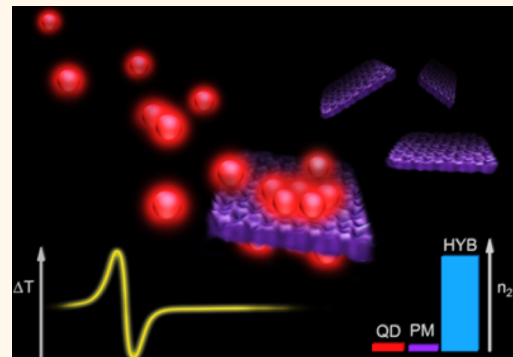


Large Enhancement of Nonlinear Optical Response in a Hybrid Nanobiomaterial Consisting of Bacteriorhodopsin and Cadmium Telluride Quantum Dots

Aliaksandra Rakovich,^{†,‡,§,*} Igor Nabiev,^{§,†} Alyona Sukhanova,^{§,†} Vladimir Lesnyak,^{†,△} Nikolai Gaponik,^{||} Yury P. Rakovich,[†] and John F. Donegan^{†,‡,*}

[†]School of Physics and [‡]CRANN Research Centre, Trinity College Dublin, Dublin 2, Ireland, [§]Laboratory of Nano-Bioengineering, Moscow Engineering Physics Institute, 115409 Moscow, Russian Federation, [†]Technological Platform Semiconductor Nanocrystals, Institute of Molecule Medicine, Trinity College Dublin, Dublin 8, Ireland, ^{||}Physical Chemistry, Technical University of Dresden, 01069 Dresden, Germany, and [△]Centro de Fisica de Materiales (CSIC-UPV/EHU) and International Physics Center (DIPC), Donostia-San Sebastian, IKERBASQUE, Basque Foundation for Science, Bilbao, Spain [#]Present address: EXSS group, Physics Department, Imperial College London, UK. [△]Present address: Istituto Italiano di Tecnologia, Via Morego 30, 16163 Genova, Italy.

ABSTRACT We report wavelength-dependent enormous enhancement of the nonlinear refractive index of wild-type bacteriorhodopsin in the presence of semiconductor quantum dots. The effect is strongest in the region just below the absorption edge of both constituents of this hybrid material and in samples that show strong Förster resonance energy transfer. We show that enhancements of up to 4000% can be achieved by controlled engineering of the hybrid structure involving variations of the molar ratio of the constituents. This new hybrid material with exceptional nonlinear properties will have numerous photonic and optoelectronic applications employing its photochromic, energy transfer, and conversion properties.



KEYWORDS: quantum dot · bacteriorhodopsin · purple membranes · D96N mutant · white membranes · hybrid material · nonlinear refractive index · nonlinear optical properties · Z-scan

Increasing energy demands by both developing and developed countries, the drive for technological advancement, and the concurrent ever-approaching limits of the semiconductor industry have all made the development of new functional materials one of the most crucial challenges of today. This demand has inspired scientists to expand their research beyond the standard materials and techniques toward multidisciplinary directions. Of particular interest are the highly multidisciplinary, and significantly more complex, bioinspired technologies based on the development of nano-bio hybrid materials. Advances to develop such hybrid materials lead to the reappearance of a photochromic protein, bacteriorhodopsin (bR)—one of the most promising candidates for industrial applications in the 1980s. Its popularity was

both due to its photochromic and photoelectric properties and also due to its chemical, thermal, and photostabilities.¹

bR is the only integral membrane protein found in the purple membranes (PMs) of bacteria *Halobacterium salinarum*, where bR's trimers form a unique nanocrystalline hexagonal array.^{1,2} This highly ordered crystalline structure protects the functional part of the protein from an aggressive external environment, including high temperatures, extreme pH values, and ionic strengths,² and is the root of this protein's exceptional stability. Upon absorption of light, bR transports a proton from the intracellular to the extracellular side of the membrane. The transport of the proton occurs through a series of optically distinguishable steps, or intermediate states, involving changes

* Address correspondence to a.rakovich@imperial.ac.uk, john.donegan@tcd.ie.

Received for review October 26, 2012 and accepted February 28, 2013.

Published online February 28, 2013
10.1021/nn3049939

© 2013 American Chemical Society

in molecular conformations of the main light-absorbing element of the protein—the retinal molecule (vitamin A aldehyde).^{1–5}

Bacteriorhodopsin films show a significant nonlinear absorption and refraction response under illumination.^{6–10} Both linear and nonlinear optical effects can be attributed to the different conformations of the bR intermediate states. The small changes of the crystalline structure of bR upon illumination as well as the accompanying shifts in electron density result in significant changes in dipole moments with subsequent shifts of bR absorption band and also changes in its refractive index.⁹ These properties can be exploited for a variety of optical applications, such as optical limiting and several types of holographic applications.^{10–13}

Recently, this technologically promising protein was used to develop new nano-bio hybrid material with high-yielding potential.^{14–17} It was demonstrated that the nanoscale interactions between semiconductor quantum dots (QDs) and bR protein within PMs in the form of Förster resonant energy transfer (FRET) lead to an improvement of the biological response of bR.¹⁵ The reported highly efficient FRET between QDs and bR indicates that significant improvement of the photoelectric and photochemical properties of bR can be achieved. Indeed, up to a 35% increase in the photoelectric response of bR films by the addition of QDs was recently demonstrated,¹⁸ paving the way for advanced nanosensing applications. However, even more attractive is the possibility to modify the photochromic properties of bR, which are inherently connected to the strong nonlinear properties of this protein. The unorthodox idea that FRET-based improvement of the biological response of the bR in the presence of QDs should influence the nonlinear properties of the bR has not been looked at so far. The feasibility of this approach to develop highly nonlinear nano-bio hybrid structures operating in the FRET regime is the focus of present work, where we detail our careful investigations of the nonlinear properties of bR/QD system using a femtosecond Z-scan technique.

RESULTS AND DISCUSSION

The hypothesis that FRET-based enhancement of the biological response of bacteriorhodopsin in the presence of QDs can translate into an enhancement of its nonlinear optical properties was tested for a system which consisted of a bR/QD hybrid material assembled from the PMs and thioglycolic acid (TGA)-stabilized CdTe QDs emitting at ~650 nm. This QD sample was chosen because it displayed efficient FRET coupling to the retinal molecule in the bR protein (see Figure S4 in Supporting Information). This sample also had relatively high extinction coefficients (Figure 1) due to the large size of the QDs. The effect of the addition of QDs on the nonlinear optical properties of PMs was investigated through comparative studies involving Z-scans of pure QD

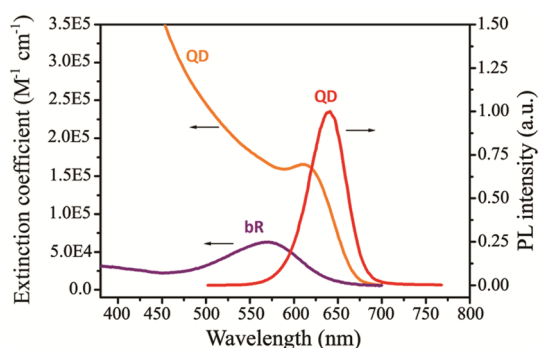


Figure 1. Comparison of spectral properties of QD650 and bacteriorhodopsin (bR) within purple membranes (PMs). The extinction coefficient of the QD sample, used in the study of the NLO properties of QD/PM complexes, is much higher than that of the retinal molecule of the bR protein. The absorption band of the retinal molecule has significant spectral overlap with the QD650 emission spectrum (red curve).

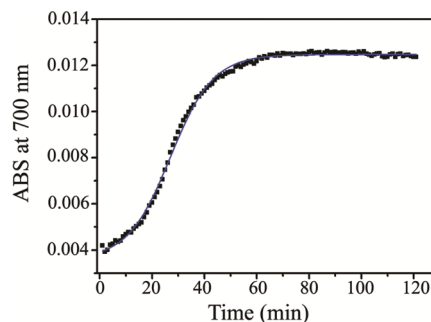


Figure 2. Self-assembly of PM/QD650 complexes monitored by transmission measurements. Scattering from the 0.5 bR-to-QD hybrid increased as the QDs and bR are assembled in solution. Scattering reached saturation after ~1 h, corresponding to the end of the assembly process. It then remained nearly constant for at least another hour. The scatter points are the experimental data; solid line is a guide for the eye.

solutions, PM suspensions without QDs, and aqueous solutions of the assembled hybrid PM/QD material.

The PM/QD hybrids were self-assembled and purified as described in Methods. The assembly was monitored by absorbance measurements at wavelengths above the QDs and bR absorption edges. No new absorption features are expected at long wavelengths since this is a hybrid material rather than one in which new compounds are formed. At these longer wavelengths, the main contribution being measured by means of absorption or transmission spectroscopy is scattering, which has a strong dependence on the average size of the particles. Temporal absorption measurements of PM/QD complexes at 700 nm showed increased scattering by the self-assembling complexes (Figure 2). The scattering reached saturation after ~1 h, corresponding to the end of the assembly process of the hybrid materials and remained nearly constant thereafter. Note that the transmittance of this sample was 97.2% (1 cm path length), and in Z-scan measurements, the transmittance value for all samples was never below 90% (1 mm path length).

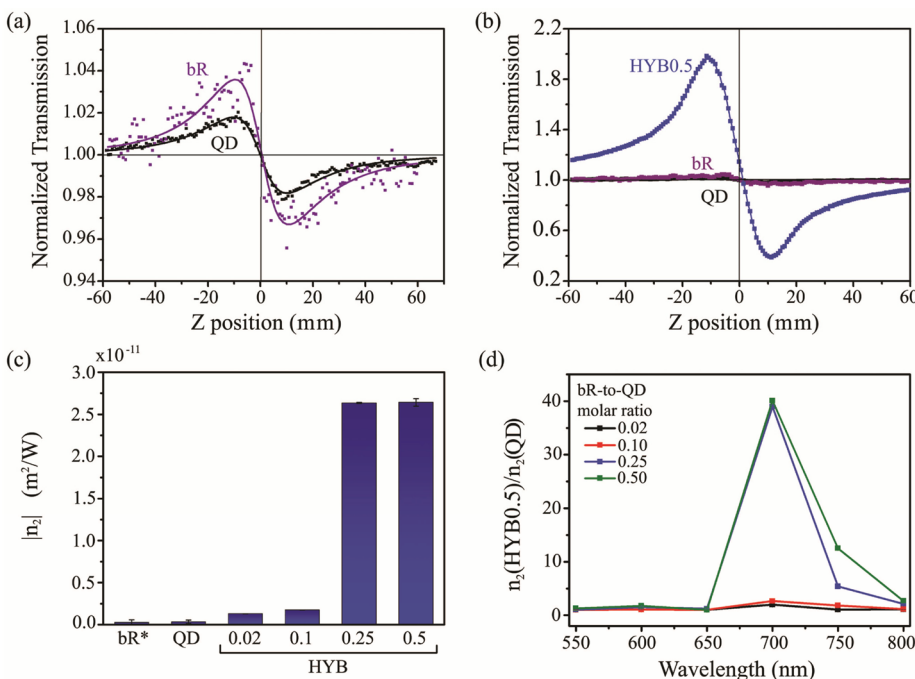


Figure 3. Enhancement of nonlinear optical properties in PM/QD hybrid. (a) Z-scans of a PM suspension (0.5 μM bR concentration, blue data points) and QD solution (black squares, 1 μM) at 700 nm wavelength. The solid curves are fits to the experimental data. (b) Comparison of Z-scan curve for 0.5 bR-to-QD hybrid (HYB0.5, blue) and Z-scans of the components. (c) Nonlinear refractive indices of bR, QD, and four of PM/QD complexes of different bR-to-QD ratios (labeled HYB, followed by the bR-to-QD ratio). An increase of n_2 was obtained for all bR-to-QD ratios, with maximum increases for bR-to-QD ratios above 0.2. The concentration of QDs was the same in all complexes (1 μM). (d) Wavelength dependence of nonlinear refraction properties of PM/QD complexes.

Temporal photoluminescence (PL) measurements showed increasing quenching of QD luminescence as the assembly of PM/QD complexes neared completion (Figure S4 in Supporting Information), which is in line with our previous observations of strong FRET coupling between QDs and bR^{14,15} and with results of the scattering measurements (Figure 2). More notably, these measurements revealed the molar ratio dependence of the strength of optical interactions in this nano-bio hybrid. Efficient FRET coupling was achieved for bR-to-QD ratios as small as 0.2, and for a 0.5 bR-to-QD sample, complete quenching of QD fluorescence was achieved in a matter of seconds (Figure S4). In view of this, four bR-to-QD molar ratios were chosen (0.02, 0.1, 0.25, and 0.5) for Z-scan measurements, to cover a range of ratios for the hybrid formation.

The Z-scan measurements were performed on a 130 fs laser system that could be tuned from 550 to 800 nm (for more details, see the Methods section and Figure S5 in Supporting Information showing a schematic of the Z-scan setup). Measurements were carried out with an excitation intensity of about $4 \times 10^3 \text{ W/cm}^2$.

Closed-aperture Z-scans of a pure QD solution and a PM suspension showed that both of these samples displayed negative lensing (Figure 3a), in agreement with the previous reports.^{2,6,19} The nonlinear refractive index (n_2) of the QD sample was estimated to be between -3.3×10^{-13} and $-6.5 \times 10^{-12} \text{ m}^2/\text{W}$ (depending on the laser wavelength), compared to a value

of $-7.2 \times 10^{-13} \text{ m}^2/\text{W}$ at 532 nm, reported by Abd El-sadek *et al.*²⁰ The nonlinear refractive index of a PM suspension (without QDs) was estimated to be between -1×10^{-14} and $-8 \times 10^{-13} \text{ m}^2/\text{W}$, which is in good agreement with previous studies of nonlinear optical parameters of a solution of free retinal molecules (n_2 values in the range of -3.9×10^{-14} to $-7.8 \times 10^{-13} \text{ m}^2/\text{W}$ at the same laser wavelength).⁷

First measurements of the nonlinear optical properties of the PM/QD hybrid material were performed at a wavelength of 700 nm, which is just above the absorption band edge of both bR and QDs. Upon self-assembly of the bR and QDs samples, there was a significant increase in the transmittance variations measured during Z-scans, which corresponds to a considerable increase in the nonlinear refractive index of the PM/QD system (panels b and c in Figure 3). For example, for the 0.5 bR-to-QD sample, $|n_2|$ increased from $6.07 \times 10^{-13} \text{ m}^2/\text{W}$ for the QD solution to $1.32 \times 10^{-11} \text{ m}^2/\text{W}$. This is equivalent to ~ 20 - and 40-fold increase of the nonlinear refraction index of the PM suspension and the QD solution, respectively. This value of n_2 is indeed quite large and compares with a similar value recently measured in graphene.²¹ Enhancement of n_2 was significantly lower for PM/QD complexes with bR-to-QD molar ratios below 0.2 (Figure 3c), as would be expected.

On the basis of the above results and our previous FRET studies,¹⁵ it is clear that we are dealing with a

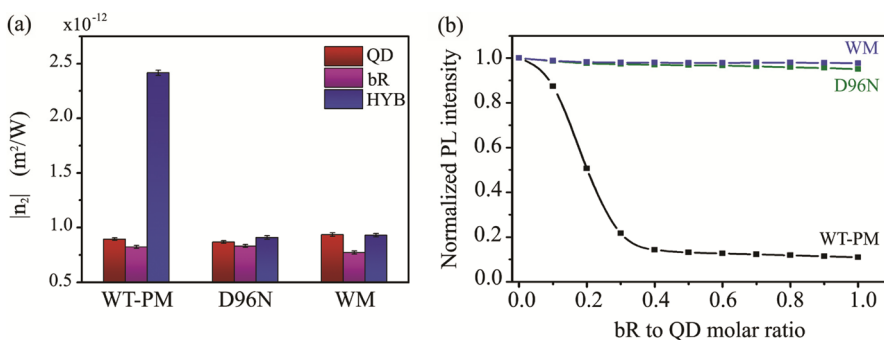


Figure 4. Enhancement of n_2 for different types of bacteriorhodopsin (bR) protein. (a) Enhancement of n_2 was found to depend strongly on the type of the bR used. Only with wild-type bR (WT-PM) was a significant enhancement obtained. For a mutant bR (D96N) and white membranes (WM), very little and no enhancement was observed, respectively. This corresponds well with the photoluminescence quenching data for these three types of bR, shown in panel (b).

system in which the two components are strongly interacting. The nonlinear optical (NLO) properties of bR are derived from the different absorption and refractive properties of its intermediate states.⁹ Therefore, any interactions leading to changes in its structure, chemical environment, and excitation state can result in changes to its photocycle and consequently its NLO properties. It is important to note, however, that many physical phenomena, including optical coupling, show very strong dependence on the frequency of incident light. Chemical effects, on the other hand, typically show limited response to it. Accordingly, we extended the measurements of the NLO properties of our nano-bio hybrid material to spectral regions above and below 700 nm.

The wavelength dependence of the ratio of n_2 for the hybrid to that of the bare QDs sample is shown in Figure 3d. This figure shows that there is a strong resonant effect just below the absorption edge of the bR and QD samples (*i.e.*, at 700 nm). Above this wavelength, the enhancement of nonlinear refraction diminishes strongly with increasing wavelength, reaching a maximum factor of only 2 at 800 nm. Remarkably, the enhancement was found to be very weak in the region where the samples absorb (<700 nm), only reaching ~80% for the 0.5 bR-to-QD sample at 600 nm. This result is noteworthy since this is the spectral region where FRET from QDs to bR ground state is very efficient.¹⁵

An interesting further experiment was to establish a correlation between the observed enhancement of n_2 at 700 nm and the efficiency of the FRET process (excitation at 480 nm) for material with the 0.5 bR-to-QD molar ratio. In order to achieve this, experiments were performed involving hybrid complexes composed from three different types of bR protein. In particular, n_2 enhancement was compared for complexes containing QDs and wild-type (WT) bR, white membranes (WM, which are native PMs with carefully extracted retinal), and a D96N bR mutant. The D96N bR mutant was chosen because it was found to be a very inefficient acceptor of the energy from QDs (see Figure 4b), while in the WM-QD system, the energy transfer does not take place at all due to the absence of

the acceptor—the retinal molecule.¹⁵ It was found that only the complex containing QDs and WT bR, in which FRET is very efficient (Figure 4b, black data points), showed a measurable increase in n_2 (Figure 4a). The change in n_2 value for the D96N mutant was only on the order of a few percent (Figure 4a), correlating well with the inefficient quenching of QDs' PL within this particular hybrid (Figure 4b, green data points). Finally, no measurable enhancement in n_2 was observed for the QDs assembled on WMs (Figure 4a), in agreement with the lack of FRET in this hybrid (Figure 4, blue data points).

The results of the experiments on the WT bR-QD system show that this hybrid nano-bio structure exhibits a large enhancement of the nonlinear refractive index over its constituents. The effect is strongest in the region just below the absorption edge of both constituents of the material and in samples that show strong FRET. Although clearly the retinal molecule that is central to FRET must also be important to the enhancement of the NLO properties in this hybrid material, there are other factors which we have to take into account to explain the observed effects. The enhancement of nonlinear polarization in the hybrid system causing corresponding enhancement in n_2 can be efficiently driven through the QDs, which may exhibit two-photon-induced PL when excited below the band gap where absorption is very low. Some degree of asymmetry in Z-scan curves and the fact that the peak intensity in our experiments is close to $4 \times 10^3 \text{ W/cm}^2$, both imply the presence of nonlinear absorption. It is noteworthy that the two-photon absorption cross section of QDs is very big, reaching 4000 GM for CdTe nanocrystals of similar size²² (which is much bigger than that of bR (290 GM⁵)) and makes two-photon excitation of QDs' PL very efficient. Using fitting procedure described in Methods and eq 5, we obtained the nonlinear absorption index of the QD sample ($\beta = -(6.3 \pm 0.2) \times 10^{-7} \text{ m/W}$), which is close to the previously reported value (*e.g.*, $-1 \times 10^{-6} \text{ m/W}$ in ref 20).

Moreover, it is important to note that the PL band of QD strongly overlaps with the absorption band of

the relatively long-lived O intermediate in the bR photocycle centered at 640 nm.⁵ This intermediate state has the highest molar absorptivity among all intermediates in the bR photocycle and, under 690 nm illumination, produces a long-lived P-state and metastable Q-state.⁵ Thereby we explain our experimental findings as a result of FRET from two-photon-excited QDs to the O-state in the bR cycle (possibly followed by a transfer of excitation to P- and Q-state), thus contributing to the enhancement of nonlinear polarizability. Further support for this mechanism comes from the observation that exactly at 700 nm, where increase in n_2 is strongest (Figure 3d), spectral overlap between the O-state and bR ground is reduced to almost zero,⁵ separating this intermediate energetically from the bR main photocycle and preventing direct transfer of the energy back to the bR ground state. However, at the same time, due to size distribution of nanocrystals in the QD sample, there is still some overlap of QD emission with bR ground state absorption, which allows one to initiate the main bR photocycle and to produce the O-state.

From our previous work,²³ it follows that, when assembled, QDs are located on the surface of PM at a distance of about 2.5 nm from the location of the retinal molecule within the PM. Both highly efficient FRET and the nonlinear optical behavior indicate that, indeed, QDs and the retinal molecule must be in intimate contact, providing the best conditions for an efficient FRET.

CONCLUSIONS

In conclusion, we have demonstrated that QDs assembled on the surface of the purple membranes containing bR are able to strongly (up to 4000% at 700 nm) enhance the nonlinear refractive index of

wild-type bR. The enhancement of nonlinear refractive index was significantly smaller at higher wavelengths and only 10–25% in the region of linear absorption (500–650 nm). We have finally clearly demonstrated that the bR, being a part of an engineered PM/QD hybrid material, is able to utilize the harvested energy to improve its nonlinear optical properties.

Our results indicate that both in the linear and the nonlinear regime the QDs and the bR represent a highly interacting system, and as such, their hybrid material is a good candidate for utilization in device applications. The technological applicability of the bR protein as a nonlinear optical material has already been established—its use in spatial light modulators, binary all-optical logical gates, frequency doubling and electro-optic devices, and in optical limiters is extensively documented in the literature.^{24–30} The enhancement of the optical properties of this protein, and control thereof, by addition of nanomaterials can aid its introduction into mass production technologies and has a profound impact on the development of next-generation photonic materials.

Further studies will be required to develop a full understanding of the extraordinary optical properties of the nano-bio hybrid. In particular, a useful follow-up to this work would be to examine the nonlinear properties of bR-QD hybrid material that consists of QDs of different sizes (different emission wavelengths) which would provide the possibility of coupling the electronic states of QDs to various intermediates of the bR photocycle. Transient spectroscopy measurements have the potential to determine the physical processes in the observed enhancement effect.

METHODS

Materials and Their Initial Characterization. Wild-type bacteriorhodopsin and D96N bacteriorhodopsin mutant, both in powder form, were bought from MIB GmbH. Prior to use, bR was dissolved in deionized water and sonicated for 60 s. bR concentration was determined from absorption measurements at 570 nm, using an extinction coefficient of 63 000 M⁻¹cm⁻¹.

White membranes (WMs) were produced using a protocol adapted from ref 31. Briefly, a suspension of PMs in 0.3 M hydroxylamine was illuminated with white light until the Schiff base, which connects the retinal molecule to the bR protein, was entirely reduced. The WMs were then separated from solution containing the retinal *via* centrifugation in the presence of human serum albumin, followed by several washing steps. The concentration of WMs prepared by this method was taken to be the same as that of the original PM sample.

QDs were synthesized using a method first developed by Rogach *et al.*^{32,33} The average core diameter of QDs in the sample (in nm) was determined according to Yu *et al.*,³⁴ based on the absorption value (A_{exc}) at the position of the excitonic peak (λ_{exc} in nm):

$$D(\text{nm}) = (9.8127 \times 10^{-7})\lambda_{\text{exc}}^3 - (1.7147 \times 10^{-3})\lambda_{\text{exc}}^2 + (1.0064)\lambda_{\text{exc}} - (194.84) \quad (1)$$

This value of QDs' average diameter was compared to that obtained using a sizing curve in ref 33, which was developed for the specific type of QDs used in this work. If significantly

different, the latter value (from the sizing chart) was used in consequent calculations.

The extinction coefficient of a QD sample was calculated from the value of the average physical diameter (D , in nm) of QDs obtained in eq 1 and the transition energy (ΔE , in eV) corresponding to the first absorption peak using the following empirical equation:²

$$\varepsilon(\text{M}^{-1}\text{cm}^{-1}) = 3450 \Delta E D^{2.4}$$

Using the measured value of absorption at the first excitonic peak (λ_{exc}) and the extinction coefficient as calculated above, the concentration of the diluted QD solution was determined through the Beer–Lambert law ($A = \varepsilon CL$, with a small correction to account for the size distribution of QDs in the sample, determined by the value of the fwhm of the emission peak (PL_{fwlm}):

$$C = \frac{A_{\text{exc}} \times (\text{PL}_{\text{fwlm}}/K)}{\varepsilon \times L} \quad (3)$$

Here, K is the correction constant which is equal to 29 for CdTe QDs.

Assembly of PM/QD in Solution. For assembly, PM and QD stock solutions were sonicated for 1 min. Different amounts of PMs were then added to the QD stock to discretely vary the bR-to-QD molar ratio of the assembled complexes. The mixed PMs

and QDs were allowed to self-assemble for 60 min under gentle agitation at ambient conditions. Assembly of WMs and D96N bR mutant with QDs was performed in a similar manner.

Z-Scan Measurements. A description and a comprehensive overview of this technique can be found in the literature.^{8,35–39} A diagram of the Z-scan setup can be found in Supporting Information (Figure S5). Z-scan measurements were performed at several wavelengths, using a LTS150 motorized stage (ThorLabs). The laser beam was focused and collimated by biconvex spherical lenses (ThorLabs). The wavelength of the pulsed laser beam from a Verdi V10 laser (<130 fs, 80 MHz, Coherent) was set to 550–800 nm using the Mira 900/Mira-OPO system (Coherent). The power of the incident beam was adjusted using a series of neutral density filters (NT59 series, Edmund Optics). The powers of the reference beam and the transmitted measurement beam were measured using two silicon photodiodes (SM05PD1B, ThorLabs) amplified by two photodiode amplifiers (PDA200C, ThorLabs). Three hundred microliters of sample at pH 7 to be analyzed was placed into a 1 mm thick high-grade quartz cuvette (Helma) and then positioned onto the moving stage. The reference and transmitted powers were recorded as a function of sample position using a LabView program that incorporated the ThorLabs software for the stage. The measured transmitted power was first corrected for laser fluctuations by dividing it by the power of the reference beam. After being normalized to transmission at the $Z = 0$ position, the corrected Z-scan trace was fitted to eq 4⁴⁰ to extract the values of phase changes due to the nonlinear properties.

$$T(x) = 1 + \frac{2(-\rho x^2 + 2x - 3\rho)}{(x^2 + 9)(x^2 + 1)} \Delta\Phi_0 \quad (4)$$

Here, $x = Z/Z_0$, where Z is the position of the sample relative to focal plane and Z_0 is the diffraction length of the focused beam ($=k(w_0)^2/2$), where $k = 2\pi/\lambda$ is the wavevector and w_0 is the radius of the beam waist, ρ is a parameter that relates the phase changes caused by nonlinear absorption ($\Delta\Psi_0$) and nonlinear refraction ($\Delta\Phi_0$) or, equivalently, the nonlinear absorption and nonlinear refraction (n_2) indices:

$$\rho = \frac{\Delta\Psi_0}{\Delta\Phi_0} = \frac{\beta}{2kn_2} \quad (5)$$

All results of Z-scan experiments were completely reproducible in multiple measurements using the same sample demonstrating high stability of the hybrid system.

Spectroscopic Measurements. A Varian Cary50Conc UV–visible spectrophotometer was used to record absorption (and scattering) spectra. Samples being analyzed were diluted until their concentration was on the order of 1 μM to avoid reabsorption effects.

Steady-state PL measurements in the UV and visible wavelength ranges were carried out using a Varian CaryEclipse fluorescence spectrophotometer. After the measurements, the raw PL data were corrected for inner filter and reabsorption effects, both of which can cause a decrease in emission intensity, unrelated to the quenching effects caused by charge or energy transfer.⁴¹ The correction was achieved by introducing a correction factor k , such that

$$\text{PL-normalized,corrected} = k \frac{\text{PL}_{\text{DA}}}{\text{PL}_D} \quad (6)$$

Here PL_{DA} and PL_D are the PL intensities of a donor–acceptor (DA) mixture and a pure donor (D) solution, respectively. The correction coefficient k was calculated according to the following equation:

$$k = \frac{(1 - 10^{-A_D^{\text{exc}}})(1 - 10^{-A_D^{\text{emiss}}})}{A_D^{\text{exc}} \cdot A_D^{\text{emiss}}} \times \frac{A_{\text{DA}}^{\text{exc}} \cdot A_{\text{DA}}^{\text{emiss}}}{(1 - 10^{-A_{\text{DA}}^{\text{exc}}})(1 - 10^{-A_{\text{DA}}^{\text{emiss}}})} \quad (7)$$

where the absorbances of the DA and D solutions and those of donor–acceptor mixtures are defined as usual:

$$\begin{aligned} A_D^{\text{exc}} &= \varepsilon_D(\lambda_{\text{exc}}) \cdot C_D \cdot L \\ A_D^{\text{emiss}} &= \varepsilon_D(\lambda_{\text{emiss}}) \cdot C_D \cdot L \\ A_{\text{DA}}^{\text{exc}} &= [\varepsilon_D(\lambda_{\text{exc}}) \cdot C_D + \varepsilon_A(\lambda_{\text{exc}}) \cdot C_A] \cdot L \\ A_{\text{DA}}^{\text{emiss}} &= [\varepsilon_D(\lambda_{\text{emiss}}) \cdot C_D + \varepsilon_A(\lambda_{\text{emiss}}) \cdot C_A] \cdot L \end{aligned} \quad (8)$$

where ε_D and ε_A and C_D and C_A are the extinction coefficients and concentrations of donor and acceptor solutions, respectively; λ_{exc} is the excitation wavelength at which the PL spectrum was measured, and λ_{emiss} is the wavelength at the PL peak.

Conflict of Interest: The authors declare no competing financial interest.

Acknowledgment. This work was funded by the Irish Research Council for Science, Engineering, and Technology (ICSET) under the Embark Initiative and by Science Foundation Ireland under Grant No. 08/IN.1/11862. Partial support of the Ministry of Higher Education and Science of the Russian Federation under the Contract Nos. 8842 and 11.G34.31.0050 is also acknowledged. Authors are grateful to Prof. S. Haacke for useful discussions, and to Dr. J.-J. Wang for experimental assistance.

Supporting Information Available: Characterization of bacteriorhodopsin samples, QD synthesis and characterization, fluorescence quenching in FRET regime, additional Z-scan information. This material is available free of charge via the Internet at <http://pubs.acs.org>.

REFERENCES AND NOTES

- Hampp, N.; Oesterhelt, D. Bacteriorhodopsin and Its Potential in Technical Applications. In *Nanobiotechnology*; Niemeyer, C. M., Mirkin, C. A., Eds.; Wiley-VCH: Weinheim, Germany, 2004; pp 146–167.
- Hampp, N. Bacteriorhodopsin as a Photochromic Retinal Protein for Optical Memories. *Chem. Rev.* **2000**, *100*, 1755–1776.
- Nuss, M. C.; Zinth, W.; Kaiser, W.; Kölling, E.; Oesterhelt, D. Femtosecond Spectroscopy of the First Events of the Photochemical Cycle in Bacteriorhodopsin. *Chem. Phys. Lett.* **1985**, *117*, 1–7.
- Mathies, R.; Brito Cruz, C.; Pollard, W.; Shank, C. Direct Observation of the Femtosecond Excited-State cis-trans Isomerization in Bacteriorhodopsin. *Science* **1988**, *240*, 777–779.
- Birge, R. R.; Gillespie, N. B.; Izaguirre, E. W.; Kusnetzow, A.; Lawrence, A. F.; Singh, D.; Song, Q. W.; Schmidt, E.; Stuart, J. A.; Seetharaman, S.; et al. Biomolecular Electronics: Protein Based Associative Processors and Volumetric Memories. *J. Phys. Chem. B* **1999**, *103*, 10746–10766.
- Aranda, F. J.; Rao, D. V. G. L. N.; Wong, C. L.; Zhou, P.; Chen, Z.; Akkara, J. A.; Kaplan, D. L.; Roach, D. F. Nonlinear Optical Interactions in Bacteriorhodopsin Using Z-Scan. *Opt. Rev.* **1995**, *3*, 204–206.
- Bezzera, A. G., Jr.; Gomes, A. S. L.; de Melo, C. P.; de Araujo, C. B. Z-Scan Measurements of the Nonlinear Refraction in Retinal Derivatives. *Chem. Phys. Lett.* **1997**, *276*, 445–449.
- Kir'yanov, A. V.; Barmenkov, Y. O.; Starodumov, A. N.; Leppanen, V. P.; Vanhanen, J.; Jaaskelainen, T. Application of the Z-Scan Technique to a Saturable Photorefractive Medium with the Overlapped Ground and Excited State Absorption. *Opt. Commun.* **2000**, *177*, 417–423.
- Sifuentes, C.; Barmenkov, Y. O.; Kir'yanov, A. V. The Intensity Dependent Refractive Index Change of Bacteriorhodopsin Measured by the Z-Scan and Phase-Modulated Beams Techniques. *Opt. Mater.* **2002**, *19*, 433–442.
- Zeisel, D.; Hampp, N. Spectral Relationship of Light-Induced Refractive Index and Absorption Changes in Bacteriorhodopsin Films Containing Wild-Type BRWT and the Variant BRD96N. *J. Phys. Chem.* **1992**, *96*, 7788–7792.
- Takei, H.; Shimizu, N. Nonlinear Optical Properties of a Bacteriorhodopsin Film in a Fabry-Perot Cavity. *Opt. Lett.* **1994**, *19*, 248–250.

12. Thoma, R.; Hampp, N.; Bräuchle, C.; Oesterhelt, D. Bacteriorhodopsin Films as Spatial Light Modulators for Nonlinear-Optical Filtering. *Opt. Lett.* **1991**, *16*, 651–653.
13. Korchemskaya, E. Y.; Stepanchikov, D. A.; Druzhko, A. B.; Dyukova, T. V. Mechanism of Nonlinear Photoinduced Anisotropy in Bacteriorhodopsin and Its Derivatives. *J. Biol. Phys.* **1999**, *24*, 201–215.
14. Rakovich, A.; Sukhanova, A.; Bouchonville, N.; Molinari, M.; Troyon, M.; Cohen, J. H. M.; Rakovich, Y. P.; Donegan, J. F.; Nabiev, I. Energy Transfer Processes in Semiconductor Quantum Dots–Bacteriorhodopsin Hybrid System. *Proc. SPIE* **2009**, *7366*, 736620.
15. Rakovich, A.; Sukhanova, A.; Bouchonville, N.; Lukashev, E.; Oleinikov, V.; Artemyev, M.; Lesnyak, V.; Gaponik, N.; Molinari, M.; Troyon, M.; et al. Resonance Energy Transfer Improves the Biological Function of Bacteriorhodopsin within a Hybrid Material Built from Purple Membranes and Semiconductor Quantum Dots. *Nano Lett.* **2010**, *10*, 2640–2648.
16. Li, R.; Li, C. M.; Bao, H.; Bao, Q.; Lee, V. S. Stationary Current Generated from Photocycle of a Hybrid Bacteriorhodopsin/Quantum Dot Bionanosystem. *Appl. Phys. Lett.* **2007**, *91*, 223901-3.
17. Griep, M. H.; Walczak, K.; Windere, E.; Lueking, D. R.; Friedrich, C. R. An Integrated Bionanosensing Method for Airborne Toxin Detection. *Proc. SPIE* **2007**, *6646*, 66460F-1.
18. Griep, M. H.; Walczak, K. A.; Winder, E. M.; Lueking, D. R.; Friedrich, C. R. Quantum Dot Enhancement of Bacteriorhodopsin-Based Electrodes. *Biosens. Bioelectron.* **2010**, *25*, 1493–1497.
19. Loicq, J.; Renotte, Y.; Delplancke, J.-L.; Lion, Y. Non-Linear Optical Measurements and Crystalline Characterization of CdTe Nanoparticles Produced by the 'Electropulse' Technique. *New J. Phys.* **2004**, *6*, 32.
20. Abd El-sadek, M. S.; Nooralden, A.; Moorthy Babu, S.; Palanisamy, P. K. Influence of Different Stabilizers on the Optical and Nonlinear Optical Properties of CdTe Nanoparticles. *Opt. Commun.* **2011**, *284*, 2900–2904.
21. Zhang, H.; Virally, S.; Bao, Q.; Kian Ping, L.; Massar, S.; Godbout, N.; Kockaert, P. Z-Scan Measurement of the Nonlinear Refractive Index of Graphene. *Opt. Lett.* **2012**, *37*, 1856–1858.
22. Pu, S.-C.; Yang, M. J.; Hsu, C.-C.; Lai, C.-W.; Hsieh, C.-C.; Lin, S. H.; Cheng, Y.-M.; Chou, P.-T. The Empirical Correlation between Size and Two-Photon Absorption Cross Section of CdSe and CdTe Quantum Dots. *Small* **2006**, *2*, 1308–1313.
23. Bouchonville, N.; Molinari, M.; Sukhanova, A.; Artemyev, M.; Oleinikov, V. A.; Troyon, M.; Nabiev, I. Charge-Controlled Assembling of Bacteriorhodopsin and Semiconductor Quantum Dots for Fluorescence Resonance Energy Transfer-Based Nanophotonic Applications. *Appl. Phys. Lett.* **2011**, *98*, 013703-3.
24. Song, Q. W.; Zhang, C.; Blumer, R.; Gross, R. B.; Chen, Z.; Birge, R. R. Chemically Enhanced Bacteriorhodopsin Thin-Film Spatial Light Modulator. *Opt. Lett.* **1993**, *18*, 1373–1375.
25. Zhang, T.; Zhang, C.; Fu, G.; Li, Y.; Gu, L.; Zhang, G.; Song, Q. W.; Parsons, B.; Birge, R. R. All-Optical Logic Gates Using Bacteriorhodopsin Films. *Opt. Eng.* **2000**, *39*, 527–534.
26. Huang, Y.; Wu, S.-T.; Zhao, Y. All-Optical Switching Characteristics in Bacteriorhodopsin and Its Applications in Integrated Optics. *Opt. Express* **2004**, *12*, 895–906.
27. Hsu, K. C.; Rayfield, G. W. Hyperpolarizability of Genetically Engineered Bacteriorhodopsin, Nonlinear Optics '98: Materials, Fundamentals and Applications Topical Meeting, **1998**, pp 322–324.
28. Groma, G. I.; Colonna, A.; Lambry, J.-C.; Petrich, J. W.; Váró, G.; Joffre, M.; Vos, M. H.; Martin, J.-L. Resonant Optical Rectification in Bacteriorhodopsin. *Proc. Natl. Acad. Sci. U.S.A.* **2004**, *101*, 7971–7975.
29. Song, Q. W.; Zhang, C.; Gross, R.; Birge, R. Optical Limiting by Chemically Enhanced Bacteriorhodopsin Films. *Opt. Lett.* **1993**, *18*, 775–777.
30. Grout, M. J. Application of Bacteriorhodopsin for Optical Limiting Eye Protection Filters. *Opt. Mater.* **2000**, *14*, 155–160.
31. Birnbaum, D.; Seltzer, S. A Highly Reactive Heteroatom Analog of Retinal and Its Interaction with Bacteriorhodopsin. *Photochem. Photobiol.* **1984**, *39*, 745–752.
32. Rogach, A. L.; Katsikas, L.; Kornowski, A.; Su, D. S.; Eychmüller, A.; Weller, H. Synthesis and Characterization of Thiol-Stabilized CdTe Nanocrystals. *Ber. Bunsen. Phys. Chem.* **1996**, *100*, 1772–1778.
33. Rogach, A. L.; Franzl, T.; Klar, T. A.; Feldmann, J.; Gaponik, N.; Lesnyak, V.; Shavel, A.; Eychmüller, A.; Rakovich, Y. P.; Donegan, J. F. Aqueous Synthesis of Thiol-Capped CdTe Nanocrystals: State-of-the-Art. *J. Phys. Chem. C* **2007**, *111*, 14628–14637.
34. Yu, W. W.; Qu, L. H.; Guo, W. Z.; Peng, X. G. Experimental Determination of the Extinction Coefficient of CdTe, CdSe, and CdS Nanocrystals. *Chem. Mater.* **2003**, *15*, 2854–2860.
35. Chapple, P. B.; Staromlynska, J.; McDuff, R. G. Z-Scan Studies in the Thin- and the Thick-Sample Limits. *J. Opt. Soc. Am. B* **1994**, *11*, 975–982.
36. Chapple, P. B.; Staromlynska, J.; Hermann, J. A.; McKay, T. J.; McDuff, R. G. Single-Beam Z-Scan: Measurement Techniques and Analysis. *J. Nonlinear Opt. Phys.* **1997**, *6*, 251–293.
37. Hughes, S.; Burzler, J. M. Theory of Z-Scan Measurements Using Gaussian-Bessel Beams. *Phys. Rev. A* **1997**, *56*, R1103–R1106.
38. Van Stryland, E. W.; Sheik-Bahae, M. Z-Scan Measurements of Optical Nonlinearities. In *Characterization Techniques and Tabulations for Organic Nonlinear Materials*; Kuzyk, M. G., Dirk, C. W., Eds.; Marcel Dekker, Inc.: New York, 1998; pp 655–692.
39. Yin, M.; Li, H. P.; Tang, S. H.; Ji, W. Determination of Nonlinear Absorption and Refraction by Single Z-Scan Method. *Appl. Phys. B: Lasers Opt.* **2000**, *70*, 587–591.
40. Ganeev, R. A.; Ryasnyansky, A. I.; Tugushev, R. I.; Usmanov, T. Investigation of Nonlinear Refraction and Nonlinear Absorption of Semiconductor Nanoparticle Solutions Prepared by Laser Ablation. *J. Opt. A: Pure Appl. Opt.* **2003**, *5*, 409–417.
41. Kubista, M.; Sjöback, R.; Eriksson, S.; Albinsson, B. Experimental Correction for the Inner-Filter Effect in Fluorescence Spectra. *Analyst* **1994**, *119*, 417–419.